THE λ10747 CORONAL LINE AT THE 1966 ECLIPSE

I: *Emission Line Polarization*

JOHN A. EDDY, ROBERT H. LEE, and JAMES P. EMERSON*
*High Altitude Observatory, National Center for Atmospheric Research,** Boulder, Colo., U.S.A.*

(Received 5 December, 1972; in revised form 12 March, 1973)

Abstract. Observations are presented of emission line resonance polarization in Fe XIII λ10747 at the total solar eclipse of 12 November 1966. Useful data, with angular resolution 15″, describe three quadrants of the corona from 1.08 $R_\odot$ to a maximum of 1.6 $R_\odot$. The direction of the electric vector of observed polarization is perpendicular to the solar limb, to the limits of accuracy of measurement, in at least 74% of all cases. Departures in the other points are consistent with the magnetic depolarization expected from the non-radial fields of streamers. Polarizations observed range from near zero at the limb to 80% and higher at 1.6 $R_\odot$. Averaged polarization is highest in non-streamer regions, where above 1.2 $R_\odot$ it suggests pure radiative excitation of the λ10747 line. Below 1.2 $R_\odot$, and in a dense streamer, the polarization is significantly depressed, indicating dominant collisional excitation of the line wherever the electron density exceeds 50×10^6 cm^{-3}.

1. Introduction

The strong coronal emission line at 10747 Å was discovered by Lyot with the coronagraph in 1936, in the course of a systematic search of the near-infrared coronal spectrum. He found it the brightest feature of the coronal spectrum in the photographic infrared, estimating its intensity to reach 240 millionths of the neighboring photospheric continuum in a bright region near the limb (Lyot, 1939). Unlike all of the other brightest coronal forbidden lines, λ10747 had to wait but three years to be identified, by Edlén, as the $^3P_1$–$^3P_0$ ground state transition of Fe XIII. The line was apparently not again observed for 20 yr after its discovery, chiefly because of the difficulty of photographic detection in the near infrared, which made observation impossible at eclipse: Lyot's 1936 plates (hypersensitized Eastman *Z* emulsion) required exposures of 4 h and longer in the coronal skies of the Pic du Midi.

Russian astronomers observed the line with image tubes at Pulkovo and Kislovodsk in 1956 (Shklovskii, 1965) and were the first to observe it at eclipse (Kurt, 1962, 1963). With a fast spectrograph, a 1 cm image tube, and exposures of 3 s, Kurt secured spectra which included the line at eight slit positions in the corona at the eclipse of 15 February 1961, from a high-flying aircraft. At its brightest, near the limb, he found the λ10747 equivalent width to be about 20 Å. Other image tube observations followed, chiefly to measure the intensity of λ10747 relative to the companion line λ10798, $^3P_2$–$^3P_1$, of the same ion (Firor and Zirin, 1962; Wlerick *et al.*, 1963; Dumont

* Present Address: Dept. of Physics, University College, London.
** The National Center for Atmospheric Research is sponsored by the National Science Foundation.

Solar Physics **30** (1973) 351–369. *All Rights Reserved*
Copyright © 1973 by D. Reidel Publishing Company, Dordrecht-Holland

and Perche, 1964; Eddy and Malville, 1967; Eddy *et al.*, 1967; Zirin, 1970; Fisher and Pope, 1971; Byard and Kissell, 1971; Ratier and Rozelot, 1972).

The $^3P_1$–$^3P_0$ transition configuration is ideal for the resonance polarization phenomenon, since the lower level has but one magnetic quantum state; atoms radiatively excited through a π or σ transition to the upper magnetic substate must return by the same π or σ transition in subsequent re-emission; hence for pure scattering, the apparent polarization of the incident radiation field in the corona (due to its directionality) is preserved in the re-emitted line. Hyder (1965) pointed out that the λ10747 line could display a maximum linear polarization of 100% at asymptotic distances above the limb, in the absence of collisions and coronal magnetic field depolarization. Thus the expected polarization in the line is, in amount, nearly equal to that of the continuum K-corona, although different in direction by 90°: in general the electric vector of resonance-polarized line emission will lie in a radial direction. The strength and anticipated high polarization in the line, and its susceptibility to the direction of the coronal magnetic field make it the most promising line in the visible and near infrared spectrum for the study of the magnetic field of the corona. A recent theoretical study of the relation between predicted λ10747 polarization and coronal conditions has been made by House (1972).

Measurements of polarization in the λ10747 line were first made at the 1965 eclipse by Eddy and Malville (1967), who observed the line photo-electrically with low spatial resolution at four points along a single position angle; they found strong linear polarization, increasing outward, with electric vector predominantly radial. At the same eclipse Hyder made measurements of the polarization in the coronal green line (Hyder *et al.*, 1968). The observations reported here, made at the eclipse of 12 November 1966, were carried out to extend the 1965 Eddy and Malville results by recording polarization amount and direction throughout the corona with improved spatial resolution. Observations of λ5303 polarization have since been made with a coronameter by Charvin (1971).

2. Apparatus

Photographs of the corona were made through an interference filter, with a polaroid analyzer which was rotated 60° between exposures – three such exposures, or filtergrams, constituting a set from which the complete description of polarization can be derived (Billings, 1966). The transmission of any filter used in this way to record line emission will include radiation from the coronal continuum, in amount dependent upon the line-to-continuum ratio and the width of the filter relative to that of the line. In the case of observations of coronal resonance line polarization this continuum component is especially important since the expected polarizations of line and continuum are generally 90° apart. It is thus crucial to subtract, as accurately as possible, the continuum component from each line filtergram. This was done in the 1966 experiment by making a set of filtergrams of the corona with the same instrument in the adjacent continuum at wavelength λ_c, and subtracting the derived continuum intensities from corresponding line filtergrams, including a correction for the difference

in the continuum level between λ_c and λ10747. The characteristics of the line (L) and continuum (C) filters used are given in Table I.

TABLE I

Interference filter characteristics

Filter	Center wavelength	Full width at half maximum	Maximum transmission	Exposure time
L	10747 Å	14 Å	41%	50 s
C	10625 Å	105 Å	68%	4.6 s

The L filter was selected for minimum bandwidth; the wider-pass C filter was chosen to permit shorter exposure times consistent with a continuum bandpass free of expected coronal or chromospheric emission features, such as the strong Helium emission at 10830 Å. The central wavelengths of both filters were checked in the eclipse instrument using an auxilarly grating spectrograph and neon line reference. The central wavelength of the L filter was maintained by temperature control.

The polaroid used was glass-mounted type HR, in a circular, rim-driven mount. The principal transmittances k_1 and k_2 of this particular sample were measured at λ_c to be 0.2172 and 0.0010. Although this makes an effective analyzer for the near infrared its relatively low total transmission $\kappa_\lambda=(k_1+k_2)/2=0.109$ is in poor contrast with that expected of commercial polaroid filters in the visible region.

The interference filters and polaroid were mounted in a collimated beam behind the focus of an f/4 reflector of 22 cm aperture. A subsequent image was formed on the face of a cooled, two-stage RCA S−1 image tube which was kindly made available to the High Altitude Observatory for this experiment by the Department of Terrestrial Magnetism of the Carnegie Institute, Washington. The image tube resolution was measured to be 25 lines mm^{-1}. An image intensifier of this type has a gain of about 160 relative to hypersentized emulsions, and an effective gain advantage of about 10 over a single-stage, S−1 image tube. The final image was recorded on IIa-0 emulsion in a 35 mm camera with a plate scale of 2.7′ mm^{-1}. A diagram of the optical system is shown in Figure 1.

The eclipse was observed at zenith angle 30° from the CV-990 jet aircraft of the NASA Ames Research Center, operating from Pôrto Alegre, Brazil and intercepting the path of totality at about 12 km altitude off the coast of Uruguay. The principal advantage of an airborne platform in the 1.06 to 1.08 μ region was in this case the extended time of totality (206 s); any gain in atmospheric transmission in this spectral region is slight. The observations were made at near-normal incidence through an aircraft window of optically polished BSc glass, 1 in. thick, chosen for optical quality and for high transmission (0.915) in the 1.08 μ region.

Airborne guidance was achieved by mounting the telescope assembly in a gimbal and inertially guiding by means of high-speed integrating gyros and brushless D.C.

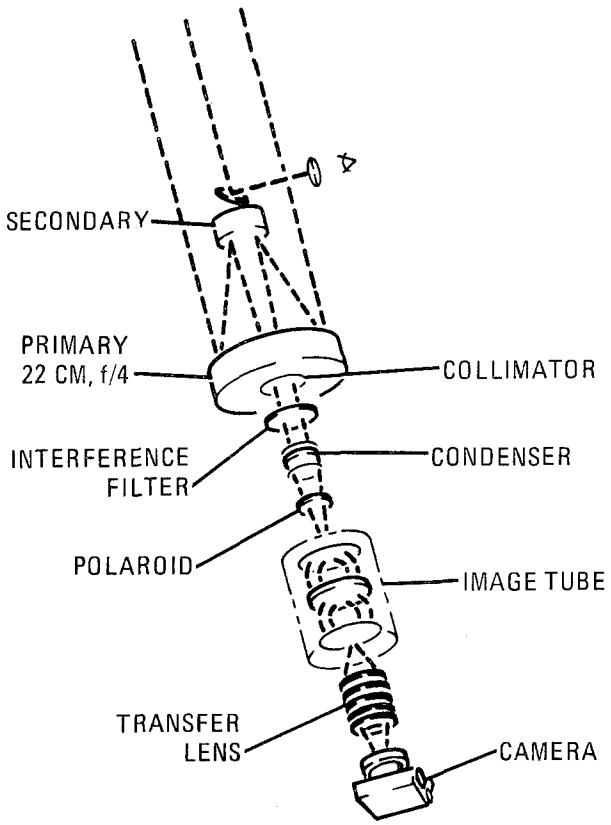

Fig. 1. Schematic diagram of optical system.

torque motors attached in two axes. In this way the telescope was pointed at the sun to an accuracy of better than $\pm 3''$, rms, throughout the period of totality – nearly as good as could have been achieved on the Earth surface. More details and a discussion of the advantages of such an inertially-guided system over other methods of airborne guidance have been discussed elsewhere (Dunn, 1966; Eddy *et al.*, 1970). A second and significant advantage of the system in this experiment was its freedom from the deleterious polarization effects of heliostat mirrors.

Instrumental polarization was expected from the interference filters and possibly the aircraft window. These effects were evaluated in the system by making airborne, calibrated exposures of the Moon near full phase through the eclipse telescope in the aircraft at the eclipse altitude. The deduced lunar polarization was then compared with that expected for the Moon at this wavelength and lunar phase, which was taken to be 1.5% (Lyot, 1929; Wright *et al.*, 1963). Results of this gave clear and unambiguous indication of instrumental polarization, different in the L and C exposures, both in amount and direction, indicating their source as due principally to the interference filters. For the L filter, the instrumental polarization was found to be 1.7%; for the

C filter, which was of poorer optical quality, 9.8%. These vector amounts were then applied as corrections to the eclipse data.

Calibration was made in units of the brightness of the spatially-averaged photospheric disk, $B_{\odot}(\lambda)$, using a diffusing opal glass filter over the telescope aperture and a series of neutral filters of known attenuation. The calibration of the opal glass and of the auxiliary filters was made subsequent to the eclipse, using the L and C interference filters to fix the wavelengths of calibration (Elmore *et al.*, 1970). Calibration exposures for the eclipse data were made in the aircraft on 14 November 1966 with the Sun within $\frac{1}{2}^{\circ}$ of its zenith distance at eclipse, and the aircraft at the eclipse altitude. The calibration film was developed with that from eclipse. Calibration exposures were of the full data frame, thus permitting point-by-point correction for the system field function, which was found to be severe because of the radial vignetting of the image tube transfer lens and the non-uniformity of the image tube response across its field. The field function was mapped and found to vary slowly across the field occupied by the coronal data, but showing a variation of as much as 55% from one side to the other. In data reduction this effect was voided by making a separate characteristic curve for each point in the field at which coronal data were obtained, statistically improving each curve by averaging nearby points in the calibration frames. Future attempts to perform coronal photometry and polarization studies with image tubes and interference filters should consider the very real limitations imposed by the non-flat field function of an image tube, non-zero polarization of interference filters, and the accumulation of errors in the plate subtraction method.

3. Observations

In the analysis, six exposures were used: three in the line of 50 s duration followed by three in continuum of 4.6 s. Filtergrams of L and C sets are similar in apperance, with only subtle differences due to polarization modulation. The polarization contrast between frames of the L set is not nearly as striking as that seen in conventional white-light continuum photographs of the corona of the corona made with polarizers. In the present case the contrast is severely affected and reduced by the varying continuum component present in the L filtergrams and the cancelling effects of L and C polarizations. Since L and C polarizations are expected to be about equal in amount but opposite in direction we expect the net observed polarization to be low. In an L frame the contribution of line emission to the total recorded intensity rises from about 15% near the limb to as much as 50% in the outer field, depending upon polaroid direction and position in the corona. Prominences which are evident along the limb in the L filtergrams are hence expected as continuum features, as are plumelike extensions at the north pole. In all L frames are evident loop structures and enhancements which are principally Fe emission features and which are very similar in appearance to those seen in λ5303 filtergrams.

Spatial resolution of the telescope/image tube system was measured to be about 15″; airborne guiding errors increased this only negligibly. Data smoothing in densito-

metry gave a final grid of points about 1′ apart along solar position angles spaced each 10°. To this scale, the change in concentricity of Sun and Moon during the eclipse was negligible. However, the apparent diurnal rotation of the position angle of the solar rotation axis is accelerated in observation from an eastward-flying aircraft, and this correction was applied, amounting to about 2°.5 of apparent solar latitude shift during the airborne totality.

The final frame of the C series was noticeably flashed by chromospheric light at the northwest limb by the premature onset of third contact in the airborne eclipse, which shortened the time of totality from an ancitipated 300 s to 206 s – about 6 s less than required for the completion of our preset, 12-exposure sequence. This effect was brought about by unexpected winds which swept the aircraft to the side and out of the eclipse corridor. The loss of one of the three continuum frames made it impossible to specify completely the continuum contribution in our L data; moreover, further reduction demonstrated that the other two C frames, and the last L frame, had been to some degree affected as the aircraft moved along the edge of the totality path during the final 20 s of the airborne eclipse. This was evident in the derived, uncorrected L polarization data as a strong, apparent polarization at the northwest limb, where third contact occurred, of a sense explained as a slight added exposure to the final L frame at this point.

Two remedies were used in the final analysis. First, the data in the northwest quadrant were rejected. Second, to specify the continuum contribution in the other quadrants we used the first C frame coupled with continuum polarization determined at the same eclipse by Saito and Hata (1970) whose region of observation coincided with ours. By this technique we assume that the polarization of the continuum is the same at 10625 Å as it is at 6200 Å; moreover, we require that the direction of continuum polarization (E vector) is everywhere tangent to the solar limb. The total intensity of the coronal continuum at 10625 Å is fixed by our one C frame, thus making allowance, in the first order, for any coronal reddening in the near infrared. Since possible reddening effects are expected to arise from predominantly unpolarized F-corona or thermal corona radiation, we are left with the polarization error in our C data which is that of the visible data, and a continuum intensity error fixed by our one C frame.

Measurements of intensity vs distance above the limb were smoothed by fitted polynomials in both line and continuum data, before the L–C subtraction process.

For the analysis of error in subsequent sections of this paper we have assumed that the accuracy of photometry in each of our frames is $\pm 10\%$.

4. Results and Interpretation

We determined the amount p and direction Ψ of polarization in the line by the relations

$$p = \frac{2\sqrt{B_1(B_1 - B_2) + B_2(B_2 - B_3) + B_3(B_3 - B_1)}}{B_1 + B_2 + B_3}$$

and

$$\Psi = \tfrac{1}{2}\tan^{-1}\left[\frac{(B_3 - B_2)\sqrt{3}}{2B_1 - B_2 - B_3}\right]$$

(Newkirk *et al.*, 1970), where Ψ is the angle between the electric vector and the direction of principal transmission of the polaroid in the initial frame, and where in each case $B = I_L - I_C$, the difference between the L exposure intensity and the (reconstructed) C exposure intensity in the same polaroid orientation. Subscripts are indices of the three polaroid positions, 60° apart.

Since a series of differences appear in these equations we must expect a large probable error to accumulate in arriving at p and Ψ. The expected accuracy of determination at any point will depend both on the basic uncertainty in the photometry of individual L and C frames, here assumed to be $\pm 10\%$, and on the relative sizes of I_L and I_C. The smallest error can be expected in places where the line contribution is largest. In these places the expected fractional standard error in our data is at best ± 0.20 in p and $\pm 20°$ in Ψ. Through a significant part of the observed coronal region the expected accumulated error exceeds the result. We have nevertheless retained all data for which the derived polarization is less than unity, since the basic error of photo-

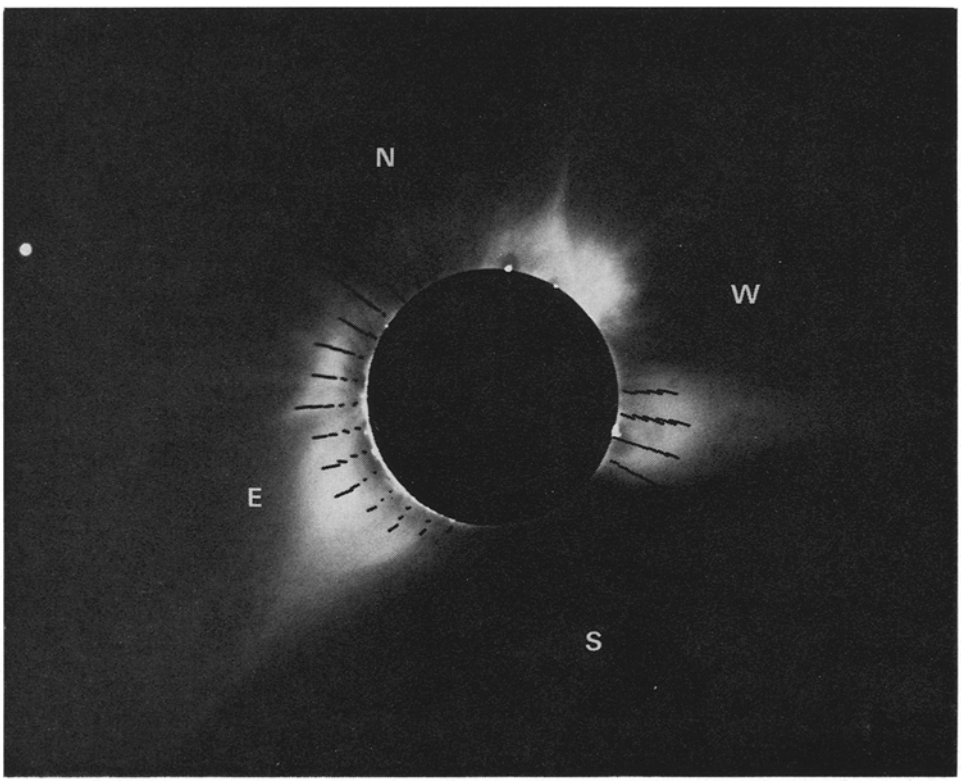

Fig. 2. Observed λ10747 polarization vectors, 12 November 1966,superposed on white light photograph by Newkirk and Lacey (Newkirk, 1967).

metry in each frame is not precisely known and because the data here are the only available, to our knowledge, on the $\lambda 10747$ polarization throughout the corona.

In Figure 2 we show the deduced polarization in the $\lambda 10747$ line superposed on a white-light photograph taken at the same eclipse, omitting the data in the northwest quadrant for the reason explained in Section C. Each line segment represents the averaged observed electric vector in $\lambda 10747$ at the position shown; the amount p and direction Ψ are represented by the length and orientation of the segment, such that $p=1.0$ is shown by a segment of length $0.2\ R_0$.

The direction of line polarization is, as expected, predominantly radial, or perpendicular to the solar limb, confirming theory and the earlier, less complete observations of Eddy and Malville (1967). The distribution of observed polarization angle about the radial direction is shown in Figure 3. In 74% of all points the observed electric vector lies less than 20° from radial, and in 55%, less than 10°. The distribution shown in Figure 3 is skewed toward positive values of ε; there would seem to be no reason

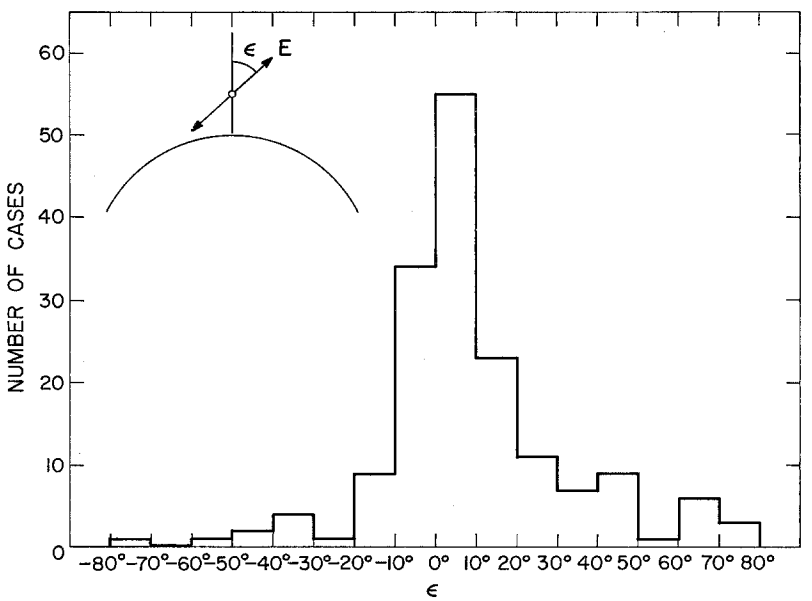

Fig. 3. Distribution of polarization angle in $\lambda 10747$: the angle ε between observed electric vector and the radial direction for all data points.

to expect a symmetrical distribution for other than simple magnetic-field cases. Even when observational errors are considered, the predominance of radial polarization direction is striking; indeed a possible interpretation of these data is that the electric vector of line polarization lies everywhere radial except in parts of the southeast and southwest quadrant where the expected coronal field might be most ordered and ideally oriented.

Throughout the corona the polarization tends to increase in amount and to become

TABLE II

Observed polarization p in λ10747, 12 November 1966

PA \ $R/R_\odot$	1.08	1.1	1.15	1.2	1.25	1.3	1.35	1.4	1.45	1.5	1.55	1.6
0°	0.32 (*0.25*)	0.34 (*0.27*)	0.37 (*0.35*)	0.46	0.75 (*0.67*)							
10°	0.49 (*0.36*)	0.51 (*0.40*)	0.66 (*0.53*)	0.89 (*0.66*)								
20°	0.37 (*0.27*)	0.52 (*0.34*)	0.75 (*0.46*)	0.59 (*0.36*)	0.62 (*0.33*)	0.92 (*0.45*)						
30°	0.18	0.14	0.26	0.50 (*0.37*)	0.68 (*0.37*)	0.74 (*0.38*)	0.79 (*0.43*)	0.96 (*0.54*)	0.97	0.95	0.95	0.94 (*0.51*)
40°	0.22	0.23	0.34	0.53 (*0.44*)	0.71 (*0.49*)	0.80 (*0.48*)	0.84 (*0.46*)	0.93 (*0.49*)				
50°	0.05	0.07	0.18	0.34	0.51 (*0.47*)	0.62 (*0.44*)	0.66 (*0.40*)	0.70 (*0.37*)	0.80 (*0.40*)	0.98 (*0.49*)		
60°	0.07	0.09	0.17	0.27 (*0.24*)	0.35 (*0.27*)	0.40 (*0.27*)	0.43 (*0.26*)	0.49 (*0.27*)	0.64 (*0.27*)	0.96 (*0.46*)		
70°	0.16 (*0.10*)	0.14 (*0.11*)	0.14	0.11	0.16 (*0.15*)	0.19	0.41 (*0.26*)	0.52 (*0.28*)	0.56 (*0.29*)	0.69 (*0.32*)	0.90 (*0.38*)	
80°	0.22 (*0.13*)	0.22 (*0.13*)	0.21 (*0.13*)	0.20 (*0.14*)	0.22 (*0.16*)	0.27 (*0.21*)	0.35 (*0.27*)	0.46 (*0.33*)	0.66 (*0.42*)	0.94 (*0.52*)		
90°	0.21 (*0.13*)	0.20 (*0.13*)	0.18 (*0.14*)	0.19 (*0.16*)	0.20 (*0.19*)	0.26 (*0.24*)	0.38 (*0.30*)	0.57 (*0.38*)	0.81 (*0.51*)			
100°	0.04	0.03	0.02	0.04	0.09	0.22	0.42	0.69				
110°	0.02	0.01	0.07	0.07	0.04	0.12	0.50 (*0.45*)					
120°	0.23 (*0.12*)	0.21 (*0.21*)	0.15 (*0.13*)	0.14	0.19 (*0.18*)	0.33 (*0.25*)	0.63 (*0.44*)					
130°	0.17 (*0.15*)	0.16 (*0.15*)	0.12	0.14	0.35 (*0.32*)							
140°	0.21 (*0.15*)	0.22 (*0.17*)	0.32 (*0.24*)	0.65 (*0.49*)								
150°	0.29 (*0.21*)	0.25 (*0.26*)	0.31									
160°	0.28	0.65										
200°	0.55 (*0.52*)	0.88 (*0.67*)										
210°	0.06	0.06	0.43 (*0.32*)	0.67 (*0.34*)	0.72 (*0.33*)	0.65 (*0.29*)	0.67 (*0.29*)	0.80 (*0.33*)				
220°	0.36 (*0.16*)	0.34 (*0.17*)	0.30 (*0.24*)	0.30 (*0.24*)	0.39 (*0.28*)	0.55 (*0.30*)	0.64 (*0.30*)	0.70 (*0.30*)	0.78 (*0.32*)	0.88 (*0.36*)	0.96 (*0.39*)	0.95 (*0.37*)
230°	0.90 (*0.38*)	0.95 (*0.39*)	0.99	0.92 (*0.40*)	0.83 (*0.38*)	0.80 (*0.36*)	0.82 (*0.34*)	0.85 (*0.33*)	0.83 (*0.33*)	0.80 (*0.33*)	0.82 (*0.32*)	
240°	0.59 (*0.13*)	0.57 (*0.14*)	0.52 (*0.17*)	0.59 (*0.24*)	0.74 (*0.32*)	0.88 (*0.39*)	0.91 (*0.41*)	0.86 (*0.40*)	0.83 (*0.35*)	0.87 (*0.33*)	0.97 (*0.36*)	
250°	0.53 (*0.17*)	0.52 (*0.17*)	0.53 (*0.19*)	0.56 (*0.70*)	0.59 (*0.21*)	0.62 (*0.24*)	0.67 (*0.29*)	0.79 (*0.34*)	0.92 (*0.34*)			

Note: Errors (standard deviations) expected on the basis of a fundamental 10% random error in each frame are shown in parentheses. Where none is given the error equals or exceeds the observed polarization value.

TABLE III

Observed $\lambda 10747$ polarization: angle ε between E vector and radial direction

PA \ $R/R_\odot$	1.08	1.1	1.15	1.2	1.25	1.3	1.35	1.4	1.45	1.5	1.55	1.6
0	+63°	+60	+47	+25	+11							
10°	+40	+36	+21	+13								
20°	+ 9	+ 6	+ 5	+ 9	+10	+ 7						
30°	+23	+13	− 5	+ 3	+ 8	+ 8	+ 6	+ 5	+7	+9	+10	+7
40°	−11	− 9	− 3	− 1	0	0	+ 1	+ 4				
50°	−14	−13	−10	− 7	− 5	− 4	− 3	− 4	−5	−6		
60°	− 3	+ 4	+12	+12	+ 8	+ 2	− 4	− 6	−5	−2		
70°	−19	−30	−43	−32	−13	− 9	− 8	− 6	−5	−5	− 5	
80°	+46	+45	+39	+32	+23	+13	+ 8	+ 5	+4	+2		
90°	+64	+60	+48	+42	+37	+30	+22	+14	+7			
100°	+76	+73	+45	+13	+ 6	+ 6	+ 7	− 8				
110°	+75	−16	+ 5	+11	+33	+21	+10					
120°	+44	+43	+36	+25	+21	+22	+20					
130°	+64	+63	+51	+28	+14							
140°	−36	−35	−27	−15								
150°	−49	−52	−12									
160°	− 9	− 3										
200°	− 4	+ 4										
210°	−78	+ 4	+ 7	+ 7	+ 6	+ 5	+ 4	+ 4				
220°	+11	+12	+11	+ 8	+ 4	+ 2	+ 1	+ 1	+2	+2	+ 3	+2
230°	− 1	− 3	− 4	− 2	0	+ 1	0	0	+2	+3	+ 1	−2
240°	+ 4	+ 5	+11	+13	+11	+ 9	+ 8	+ 7	+4	+2	+ 2	
250°	+ 7	+10	+13	+11	+ 8	+ 9	+12	+12	+7			

more nearly radial with increasing distance from the limb, as one would expect from the combined effects of the change in geometrical dilution factor and the increasing importance of radiative excitation. This trend is more clearly noted in examination of Tables II and III, which list the amount of polarization p and the angle ε for all observed points.

In the strong-field case the electric vector of resonance polarization in the coronal magnetic dipole lines should map the projected lines of the coronal field. As pointed out by a number of previous authors (Charvin, 1965; Perche, 1965; Hyder, 1965; House, 1972) this presents an opportunity to observe the configuration of the projected coronal magnetic field. Obviously our limits of accuracy preclude any detailed deductions, although it is tempting in Figure 2 to attribute the systematic and shaped trends of polarization seen at the east limb and in the southwest quadrant to the field lines one would expect in these locations from the observed streamer shapes.

Evident in these results is another antitipated effect of the coronal field: the tendency of the direction of polarization to become more nearly radial near the poles. This is apparent at position angles 10, 160, 200, and 210°, and can be explained if one assumes that the polar field is more ordered and more radially oriented.

House (1972) has carried out extensive theoretical predictions of the λ10747 polarization for the 1966 eclipse corona, including the effects of coronal density distributions derived from the white light measurements and magnetic depolarization deduced from the coronal magnetic field calculations which were made by Altschuler and Newkirk (1969) from disk magnetograms. In Figure 4 we compare one of House's

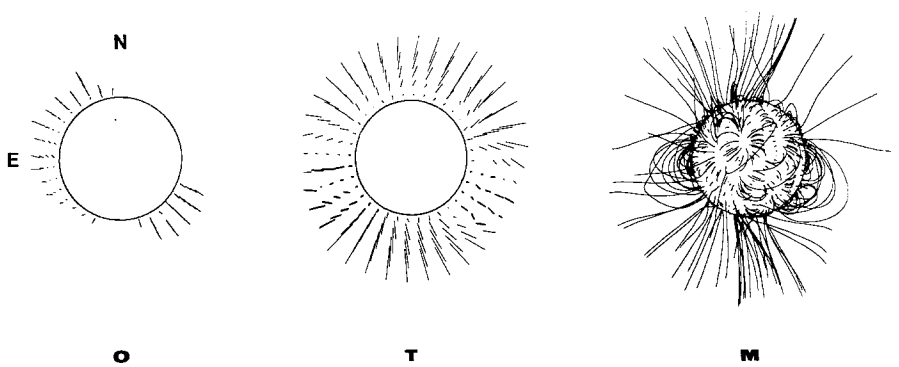

Fig. 4. Comparison of observed λ10747 polarization (O) with that predicted (T) by House (1972), with the model of the magnetic field used in his prediction (M).

predictions with our data from Figure 2. The lengths of the polarization vectors in the House prediction are scaled such that $p=1.0$ equals 1 $R_\odot$, as compared to 0.2 $R_\odot$ in the observations. It is thus apparent that the predicted polarizations are lower than the observed, indicating most probably the error in the observation. A criticism which applies to these data (and to any others from which an oppositely polarized continuum component must be subtracted) is that error in the observed L data will show up after

continuum correction as a net signal which is polarized opposite to that of the continuum – i.e., with electric vector radial to the Sun. Were our L data pure unpolarized noise, for example, the deduced net polarization in the line obtained after subtracting a wholly tangentially-polarized continuum component would be 100% polarized with radial electric vector. This effect undoubtedly explains the higher than expected line polarizations. The appearance of a number of expected polarization effects and trends in our data and the results of our rather conservative error analysis give credence to the reality of strong radial polarization in the net line data, in the face of the spectre of this rather insidious noise effect. It is clear that any future observations of emission line polarization which are to be of real use in deducing the coronal magnetic field will have to be much more carefully made, with especial attention paid to instrumental polarization effects and to the very careful measurement of the continuum intensity and polarization. This probably restricts useful measurements to those made outside eclipse.

In view of our observational error limits it does not seem useful to make more than general comparisons with House's model. Gross features which might be expected to appear in the observations are the polarization nulls which should be seen whenever the incident radiation field and the coronal magnetic field intersect at the Van Vleck angle. House has shown that for the simplified case of a global dipole field this condition will apply at each of the four position angles in the corona which are 70° from the (magnetic) poles of the Sun – i.e., at approximate position angles 70, 110, 250, and 290°. With less idealized field configurations Van Vleck nulls should still appear, in places where an ordered local field crosses the radiation propagation direction at the proper angle. In House's prediction for the 1966 eclipse, which used the potential field extension of Altschuler and Newkirk, two of these local Van Vleck nulls appear –

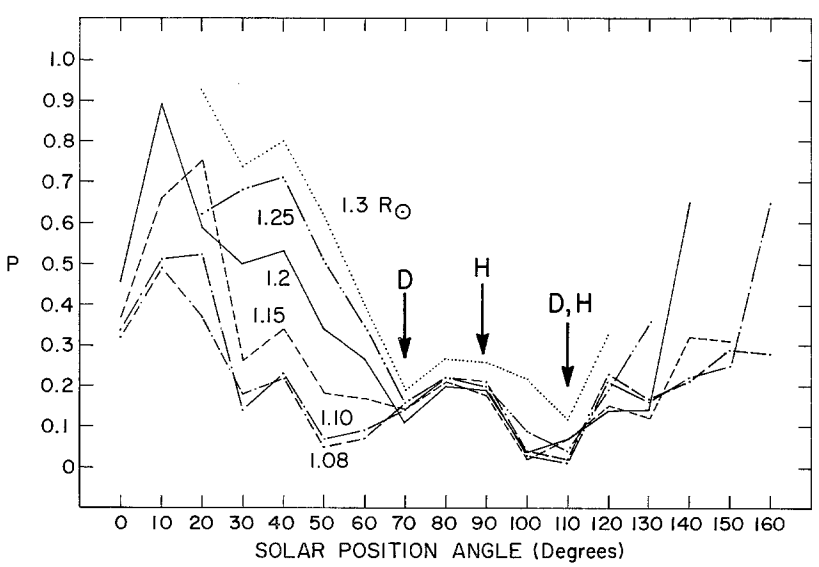

Fig. 5. Observed λ10747 polarization in the eastern coronal hemisphere.

symmetrically placed at either side of the axis of the ordered field of the southeast streamer. In Figure 5 (described below) we have marked these with letters 'H', at position angles 88 and 108°.

The predicted Van Vleck null near 108° is quite clearly present in our data, as is evident in Figure 5, where we plot observed polarization p as a function of solar position angle for the east hemisphere at six heights above the limb. Positions of nulls in the House model are shown by arrows labelled H. There seems little doubt that a minimum in polarization is observed at all heights above the limb at position angle 110°, where p reaches its minimum value in our data, 1%. The second null in the House prediction, at 88° position angle, is not observed. There appears instead another possible null at 70°, where, in the potential field extension description of the corona, the field consists chiefly of radial, open lines. Thus, of the two possible observed nulls, one is predicted by the potential field extension model, and one is not; moreover a predicted null fails to appear. Curiously the two observed nulls coincide with those expected were the coronal field a simple dipole (shown in Figure 5 with arrows marked D). The disparity between observation and the more realistic theoretical prediction of the positions of Van Vleck nulls could be taken as evidence of error in the presumed field configuration, thus casting doubt on the reliability of the potential field extension method for describing the real coronal field. It should be pointed out that the validity of the potential field extension method has yet to be conclusively established; the principal evidence for its usefulness is the apparent agreement between the appearance of many of the ordered field lines with white-light coronal structures. The Van Vleck nulls expected in coronal emission line polarization provide a more objective and quantitative check on the potential field extension method and supply a strong incentive for carrying out more careful and detailed measurements of coronal emission line polarization. The data here are only marginal for this test.

One can add credence to the observed polarization values by averaging over position angle in distinct regions. We have done this for two broad regions in the eastern hemisphere of the corona: the well-developed streamer in the southeast, averaging over position angles 70 to 150°, and the non-streamer or 'quiet corona' region in the northeast, between position angles 0 and 60°. The results are shown in Figure 6. Polarizations for the streamer are shown as open circles with error bars indicating the standard deviation (random error) of the position angle average. Because of the distinct difference in polarization near the Van Vleck position angle we omitted the data from position angles 100 and 110° in the streamer averages (circle points); the triangles are the streamer averages with 100 and 110° position angles included. We note that the effect is not major. The observed streamer polarizations may be described as rising slowly from about 20 to 25% between 1.1 and 1.3 $R_\odot$, followed by a sharp and distinct rise above this level, reaching about 80% at 1.5 $R_\odot$.

The averaged polarizations in the non-streamer region (points x in Figure 6) behave in an entirely different way, rising uniformly and rather steeply above 1.1 $R_\odot$. An observed rise in polarization with distance above the limb is expected because of the increased anisotropy of incident radiation. The form of this expected geometrical

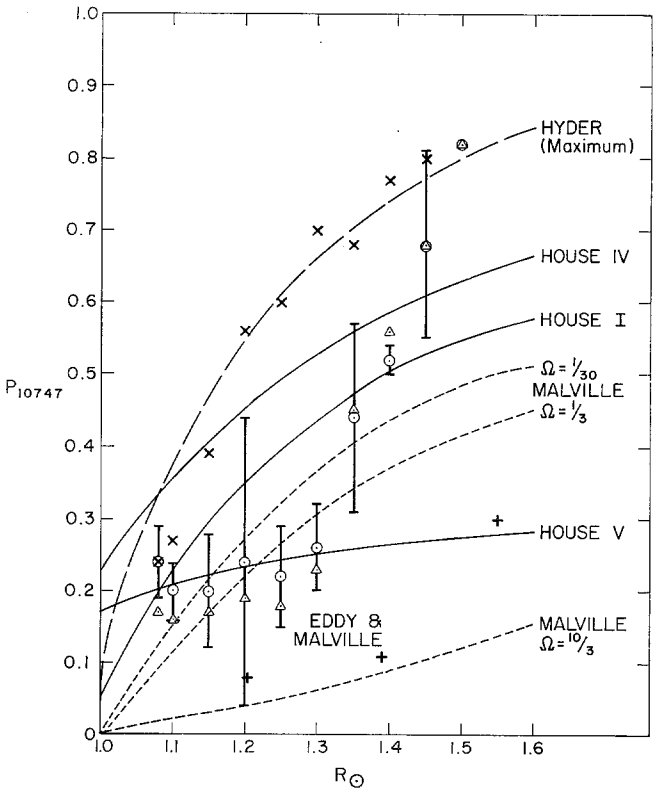

Fig. 6. Observed and predicted polarization, p, in $\lambda 10747$.

decrease is shown in the figure as a dashed curve, from an early calculation by Hyder (1965) for the case of purely radiative excitation, a two-level atom, and no magnetic depolarization. Except for a small difference in limb darkening which Hyder introduced in the calculation, this curve is perforce the same as that which describes the electron-scattered K-corona, and may be taken as an upper limit to possible observed polarization in the line. In the non-streamer case the agreement with this pure radiative curve above about 1.2 $R_\odot$ is striking.

Actual polarizations can be expected to fall below the Hyder maximum curve because of any of the following effects: collisional excitation, magnetic depolarization, or line-of-sight integration. The simplest of these to consider is that of collisional excitation, and as a first approximation we can explain the different behavior of the streamer and non-streamer curves as due to the different importance of collisions in the two regions. We can then say for the streamer case the high electron density below about 1.3 $R_\odot$ maintains collisional excitation in this region, with a transfer to dominantly radiative excitation in the line above that point. In the non-streamer region, collisional and radiative excitation combine to keep the resultant polarization below the purely radiative curve until about 1.2 $R_\odot$, when the excitation becomes almost entirely radiative. Further evidence for this shift in excitation mechanism for the

line at 1.2 to 1.3 $R_\odot$ is found in the observed gradients of line emission intensity, to be shown in a subsequent paper.

An alternate explanation for the differences in the observed polarization curves in streamer and quiet corona is in different magnetic depolarization: the stronger, more ordered field presumed to exist in the lower streamer regions may severely reduce the polarizations apparent there. Hyder (1965) has shown that the existence of a very small non-radial magnetic field can drastically alter the direction of observed line polarization – a 10^{-5} G field reducing the polarization by an order of magnitude in the optimum geometry of observation along a non-radial magnetic field line. Indeed the 1.3 $R_\odot$ limit of apparent depolarization is close to that found for the limit of non-radial field lines in a condensation by Saito and Billings (1964). Moreover the occurrence of the Van Vleck null at position angle 10° (and possibly 70°) indicates the existence of a non-radial field there. While magnetic depolarization undoubtedly contributes to the observed polarization curves, two considerations lead us to favor collisional control. One is the shape of the λ10747 emission gradients which agree with a rather definite shift to radiative excitation at 1.2 to 1.3 $R_\odot$. Another is found in noting the quite different behavior of polarization in the other distinct helmet streamer, in the southwest quadrant. While the shapes of the southeast and southwest streamers (and presumably, therefore, their magnetic field configurations) are very similar, their densities are different: the southwest streamer, which exhibits higher line polarization, has electron densities nearly two times lower than the southeast counterpart (Newkirk *et al.*, 1970; Waldmeier, 1968), suggesting the control of depolarization by electron density. If correct, this different polarization behavior provides a method for defining a threshold of electron density which separates regimes of collisional and radiative excitation in the λ10747 line. In Figure 7 we show the electron densities determined by Waldmeier (1968) for the two streamers which we have been considering. Where our line polarization data indicate collisional dominance the curve of electron density is shown as a solid line; where radiative dominance is indicated the electron density curve is dashed. In considering the figure we should recall that the polarization results were obtained by averaging over large regions of position angle. With the possible exception of the 1.1 $R_\odot$ electron density profile in the southwest streamer, the case seems made for a threshold at about $N_e = 50 \times 10^6\ \mathrm{cm}^{-3}$: for electron densities above 50×10^6 collisions are important in populating the λ10747 line; below this density, collisions may be almost entirely ignored.

These considerations permit a general comment about the coronal field. The high polarizations found in the northeast quadrant and southwest streamer, and the nearly radial direction of polarization there, suggest that magnetic depolarization effects are of minor importance in these regions. Following Hyder's reasoning, this would establish an upper limit of about 10^{-5} G for the line-of-sight component of any coronal magnetic field above about 1.1 $R_\odot$ in these two regions. This field strength is very much lower than that indicated in a review of coronal magnetic fields by Newkirk (1967).

We have included in Figure 6 several theoretical calculations of expected λ10747

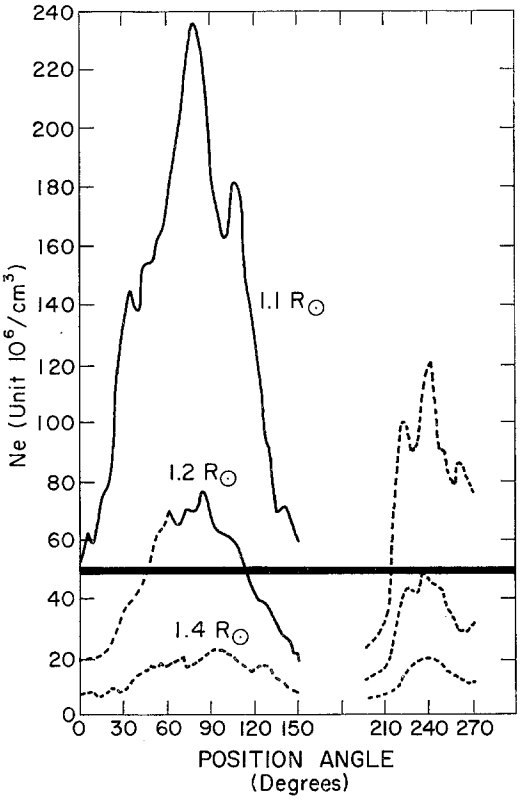

Fig. 7. Electron densities derived by Waldmeier (1968) for the southeast and southwest streamers for different heights at the 1966 eclipse.

polarization which include collisional effects. The (dashed) curves by Malville (1967) are modifications of the Hyder curve for a model coronal density and three presumed values of the collision strength Ω for $^3P_0$–$^3P_1$: 0.033, 0.33, and 3.3. In a recent review Chevalier and Lambert (1969) conclude that the most likely value is 0.049. Malville intended the curves as a device for determining the collision strength in the line through observation of the general gradient of emission line polarization. The nature of observed polarization in different coronal regions and the sharp break observed in the high electron density (streamer) curve where the line comes under the control of radiative excitation severely limit the value of this generalized comparison. Moreover Malville's calculations did not include the effects of collisional excitation from higher atomic levels nor the effects of proton-ion collisions, which were subsequently shown by Chevalier and Lambert to be at least as important as electron collisions in this transition when the temperature exceeds 10^6 K. These two effects, if included, would tend to lower Malville's curves, though not significantly for the purpose of comparison with the data shown here.

The calculations by House (1972) (solid lines in Figure 6) are more sophisticated

predictions, but again are for averaged streamer regions; again, the comparison with observation is disappointing. His Case I curve is based upon average density gradients observed at the 1966 eclipse by Newkirk *et al.* (1970), with no magnetic depolarization and no limb darkening. The curve IV is the same model with complete limb darkening, thus decreasing the effective solid angle of the source of photospheric excitation and increasing the observed polarization. Previous observations of limb darkening near 1 μ wavelength would indicate that Case I is a slightly better approximation (Pierce *et al.*, 1950). House's Case V is for the case of a constant-density corona, which produces a surprisingly good fit to our observed streamer polarization curve between 1.1 and 1.3 $R_\odot$. Since a gradient of electron density is a well-observed feature of coronal streamers, we interpret this fit as the effect of a streamer density which is much higher than the average used in House's Case I prediction, and of a balance between collisional and radiative excitation which shifts rather abruptly to dominantly radiative above 1.3 $R_\odot$ in the streamer.

The observed non-streamer curve of polarization might be expected to fit more closely House's Case I curve, since the averaged density model which he used might better pertain. Departures, however, are as striking as in the streamer case. From the limb to 1.1 $R_\odot$ the model may apply. From 1.2 $R_\odot$ outward, however, the non-streamer observations indicate a simple case of purely radiative excitation, apparently unaffected by collisional or magnetic field depolarization. At this point (1.2 $R_\odot$) the average non-streamer coronal density is very close to our empirical threshold of 50×10^6 cm^{-3} (Newkirk *et al.*, 1970). It may well be that whenever the coronal density falls below this value the λ10747 polarization will follow a purely radiative curve; when the density exceeds this limit, the polarization will be drastically and dominantly depolarized by collisions. If this is so, the deduction of coronal magnetic fields from λ10747 emission line polarization data will be more difficult than supposed in the simple cases that House considered, since the magnetic depolarization will be a second-order effect, probably inseparable from collisional depolarization below 1.1 or 1.2 $R_\odot$ and limited to a minor modulation of the radiative polarization curve above this limit.

We have also included for comparison in Figure 6 the polarizations observed at the 1965 eclipse by Eddy and Malville (1967). By their technique of measurement, with polaroid analyzers oriented in only two positions, parallel and perpendicular to the limb, the inferred polarizations are necessarily lower limits, representing the true value only when the actual vector of maximum polarization lies in one of these directions. This could explain the discrepancy between their 1965 measurements and the newer data presented here. Or their measurements, which were made in an equatorial streamer, could represent again the strong depolarization of high density regions. Perhaps the fairest comment on λ10747 polarization at this point is that the world awaits a convincing coincidence between theory and observation.

5. Summary of Results

The λ10747 line was found to show strong linear polarization with electric vector

perpendicular to the limb of the Sun in at least 74% of all observed points. In helmet streamers the electric vector has a tendency to delineate the field lines which are predicted by the surface potential field approximation, although our accuracy of measurement does not permit a detailed check of this point. The field implied by the radial polarization observed in non-streamer regions is not consistent with the potential field approximation there, either because of error in that method or due to very low field strengths. A null in polarization is observed at position angle 110° in the southeast streamer where the radiation field and the presumed streamer magnetic field cross at the Van Vleck angle, confirming a prediction by House. Another Van Vleck null appears in a non-streamer region at a position angle (70°) which is consistent with the existence of a simple, global dipole field.

The amount of polarization behaves differently in and out of strong streamers. In an averaged non-streamer region the polarization is high, and above 1.2 $R_\odot$ follows a curve expected for the case of purely radiative excitation in the line, i.e., with no collisional or magnetic field depolarization. This is consistent with the observed dominantly radial direction of polarization in this region and implies that there are no non-radial magnetic fields there with strengths greater than 10^{-5} G. The averaged polarization curve in the intense southeast streamer is considerably depressed relative to the non-streamer case, in a way that is most likely interpreted as depolarization by collisional excitation of the line. The different behavior of streamer and non-streamer average curves can be explained under the hypothesis that the line is under strong radiative control whenever the local electron density is less than about 50×10^6 cm^{-3}, and dominantly excited by collisions for densities which exceed this amount. In the quiet, or non-streamer corona this threshold is reached at 1.1 to 1.2 $R_\odot$. The effect of the coronal field on the amount of polarization appears to be a second-order effect, overshadowed by strong density effects.

A subsequent paper will treat the observations of intensity total and equivalent width in λ 10747 at the 1966 eclipse.

Acknowledgement

We are indebted to Dr M. Bader and personnel of the Airborne Science Office, NASA Ames Research Center for aircraft support, and to Dr J. W. Firor, NCAR, for assistance in taking the observations. The image tube was kindly provided by the Department of Terrestrial Magnetism of the Carnegie Institution, Washington, D.C. through the courtesy of Dr W. K. Ford, Jr. The Council of Clare College, Cambridge provided a travel grant for J.P.E. We thank Dr L. L. House for useful comments and corrections.

References

Altschuler, M. D. and Newkirk, G., Jr.: 1969, *Solar Phys.* **9**, 131.
Billings, D. E.: 1966, *A Guide to the Solar Corona*, Academic Press, p. 96.
Byard, P. L. and Kissell, K. E.: 1971, *Solar Phys.* **21**, 351.
Charvin, P.: 1965, *Ann. Astrophys.* **28**, 877.

Charvin, P.: 1971, in R. Howard (ed.), 'Solar Magnetic Fields', *IAU Symp.* **43**, 580.
Chevalier, R. A. and Lambert, D. L.: 1969, *Solar Phys.* **10**, 115.
Dumont, J. P. and Perche, J. C.: 1964, *12me Coll. Int. Astrophys. (Liège)*, p. 86.
Dunn, R. B.: 1966, *Trans. Instrum. Soc. Am.* **5**, 119.
Eddy, J. A. and Malville, J. M.: 1967, *Astrophys. J.* **150**, 289.
Eddy, J. A., Firor, J. W., and Lee, R. H.: 1967, *Astron. J.* **72**, 1352.
Eddy, J. A., Lee, R. H., Léna, P. J., and MacQueen, R. M.: 1970, *Appl. Opt.* **9**, 439.
Elmore, D. F., Streete, J. L., and Eddy, J. A.: 1970, 'Calibration of Opal Glass Attenuators', Astro-Geophysical Memorandum No. 178, High Altitude Observatory.
Firor, J. and Zirin, H.: 1962, *Astrophys. J.* **135**, 122.
Fisher, R. and Pope, T.: 1971, *Solar Phys.* **20**, 389.
House, L. L.: 1972, *Solar Phys.* **23**, 103.
Hyder, C. L.: 1965, *Astrophys. J.* **141**, 1382.
Hyder, C. L., Mauter, H. A., and Shutt, R. L.: 1968, *Astrophys. J.* **154**. 1039.
Kurt, V. G.: 1962, *Soviet Astron., Astrophys. J.* **6**, 349.
Kurt, V. G.: 1963, *Soviet Astron., Astrophys.* **6**, 620.
Lyot, B.: 1929, *Ann. Obs. Paris* **8**, 1.
Lyot, B.: 1939, *Monthly Notices Roy. Astron. Soc.* **99**, 580.
Malville, J. M.: 1967, *Astrophys.* J. **148**, 229.
Newkirk, G., Jr.: 1967, *Ann. Rev. Astron. Astrophys.* **5**, 213.
Newkirk, G. A., Dupree, R. G., and Schmahl, E. J.: 1970, *Solar Phys.* **15**, 15.
Perche, J. C.: 1965, *Compt. Rend. Acad. Sci. Paris* **260**, 6037.
Pierce, A. K., McMath, R. R., Goldberg, L., and Mohler, O. C.: 1950, *Astrophys. J.* **112**, 289.
Ratier, G. and Rozelot, J. P.: 1972, *Solar Phys.* **23**, 394.
Saito, K. and Billings, D. E.: 1964, *Astrophys. J.* **140**, 760.
Saito, K. and Hata, S.: 1970, *Ann. Tokyo Astron. Obs.*, Series II, **12**, 151.
Shklovskii, J. S.: 1965, *Physics of the Solar Corona*, Pergamon Press, p. 97.
Waldmeier, M.: 1968, *Z. Astrophys.* **69**, 193.
Wlerick, G., Dumont, J.-P., and Perche, J.-C.: 1963, in J. W. Evans (ed.), *The Solar Corona*, Academic Press, p. 177.
Wright, F. E., Wright, F. H., and Wright, H.: 1963, in B. M. Middlehurst and G. P. Kuiper (eds.), *The Moon, Meteorites, and Comets*, Univ. Chicago, Chapter 1.
Zirin, H.: 1970, *Solar Phys.* **11**, 497.